RSC Advances

PAPER

View Article Online
View Journal | View Issue

Cite this: *RSC Adv.*, 2025, **15**, 27772

Synthesis, spectroscopic studies and computational modelling of anthracene-bis-*N*-acetylglyoxylic amide derivative for anion recognition

Venty Suryanti, *[a] Hilda Alfiyani Setyono,[a] Yuniawan Hidayat,[a] David StC Black [b] and Naresh Kumar [b]

A new fluorescent anion receptor containing anthracene and amide moieties has been synthesized to selectively recognize anions *via* hydrogen bonding and electrostatic interactions. An anthracene-bis-*N*-acetylglyoxylic amide derivative, namely *N*,*N*′-(anthracene-9,10-diylbis(methylene))bis(2-(2-acetamidophenyl)-2-oxoacetamide), was successfully synthesized by reacting of 9,10-diaminomethyl anthracene with *N*-acetylisatin. An analysis of the anthracene-bis-*N*-acetylglyoxyl amide derivative's interaction with anions revealed that it recognized CN^-, F^-, and $H_2PO_4^-$ more selectively than other anions studied, such as Cl^-, NO_2^-, HPO_4^{2-}, HSO_4^-, and ClO_4^-. As shown by ^1H NMR spectroscopy data, the addition of CN^- and F^- caused the receptor to deprotonate, and that intermolecular hydrogen bonding led to the complex formation between the receptor and $H_2PO_4^-$. Based on the UV-Vis spectroscopy data, the synthesized compound's binding site and the anthracene fluorophore did not show any noticeable ground-state interactions, after adding anions. The fluorescence data revealed that the CN^-, F^-, and $H_2PO_4^-$ addition caused in an enhancement of fluorescence intensity, suggesting that the anion caused the anthracene-bis-*N*-acetylglyoxylic amide to become more rigid. Using DFT approximation, the positive surface of the molecules was identified as the most potential area for interaction with the F^- anion. Additionally, the more intense blue gradient of the non-covalent interaction spectra indicates a tendency for hydrogen bond-type interactions.

Received 14th May 2025
Accepted 27th July 2025

DOI: 10.1039/d5ra03382a

rsc.li/rsc-advances

Introduction

Considering the consequences of anions in biological, industrial processes, and environmental, synthesizing anion receptors has been fascinating for many years. The varied geometries of anion cause a challenge in anion receptor design. The anionic guest's size, shape, and charge have to complement that of the anion receptors.[1] Synthetic anion receptors have revealed many particular application potentials in the areas of anion sensors, phase-transfer catalysts, anion-selective electrodes, extraction and separation anion.[2] As anion's binding sites, N–H containing molecules, including amides, amines, ureas, sulfonamides, pyrroles, and imidazolium groups, have been utilized extensively.[3] The correct orientation of hydrogen bonds between the receptors and anions, such as N–H···anion or O–H···anion, are often exploited to fulfil this requirement. Their interactions are stabilized by hydrogen bondings.[4] The amide based on non-macrocyclic aromatic receptors have been synthesized for anion binding towards $H_2PO_4^-$, AcO^-, and Cl^-, forming complexes.[5] The complexes stability depends on the anion's basicity.

In recent years, anion recognition has advanced through deep learning-guided receptor design and water-compatible fluorescent probes with high selectivity. These approaches offer impressive sensitivity but often require complex synthesis or limited photostability. Deep learning allows researchers to move beyond traditional trial-and-error methods and develop receptors tailored to specific anions, with applications ranging from catalysis to biosensing.[6–10] Water-soluble fluorescence-based probes are used in various applications, including detecting and imaging biomolecules, ions, and other analytes in biological systems and environmental monitoring.[11–13] The research aims to obtain an anion receptor with simplicity, photostable fluorescence, and efficient hydrogen bonding that can detect a specific anion and convert the recognition event into a signal.

The amide group is a good hydrogen-bond donor group, which forms hydrogen bonds between the amide group and anions directionally, resulting in strong complexes with

[a]*Department of Chemistry, Faculty of Mathematics and Natural Sciences, Universitas Sebelas Maret, Surakarta, Jawa Tengah, 57126, Indonesia. E-mail: venty@mipa.uns.ac.id*

[b]*School of Chemistry, University of New South Wales, Sydney, NSW 2052, Australia*

anions.[4] A series of bis-*N*-acetylglyoxylic amide has been easily obtained by ring-opening bis-acylisatins with amines.[14] Bis-glyoxylamide peptidomimetics library has also been synthesized by reacting of bis-*N*-acetylisatins connected at C5 with amines.[15] The amide has been utilized as the binding site for the anion receptors. *N*-acetylglyoxylic amide derivatives **1** and **2** bearing a nitrophenyl moiety (Fig. 1) displayed CN^- and F^- recognition by hydrogen bonds.[16,17] Its color changes were ascribed to the intramolecular charge transfer that followed the N–H group's deprotonation. Multiple hydrogen bonds of N–H···Cl and C–H···Cl were found to result in a strong binding for the chloride ion in the crystal structure of *N*-nitrophenylglyoxylamide **1** when linked with TBA-Cl.[16,17] Similarly, a cinnamaldehyde derivative with a nitrophenyl moiety **3** performs color changes for the $H_2PO_4^-$ and AcO^- sensing.[18,19]

One common fluorescent signaling unit utilized to convert the binding event into a signal is anthracene. It is an ideal structure for constructing anion receptors with high-affinity binding and sensing.[20,21] It has been discovered that derivatives of anthracene are selective fluorescent chemosensors for anions.[22,23] In this study, we synthesized a new fluorescent anionic receptor, the anthracene-bis-*N*-acetyl glyoxylic amide derivative, based on the chemical characteristics of anthracene and amide. The ring opening of *N*-acetylisatin was carried out by anthracene containing amine groups. The fluorescent unit of anthracene was selected for this work as a scaffold for linkage to the N–H binding site of glyoxylamide. The anthracene-bis-*N*-acetylglyoxylic amide, which has four N–H groups, was predicted to establish several strong hydrogen bonds with anions for increased binding selectivity and affinity. Titration experiments were used to investigate the interaction between the synthesized compound and anions which were monitored by UV-Vis, fluorescence, and ^{1}H NMR spectroscopy.

Meanwhile, density functional theory (DFT) in molecular modeling has become a powerful tool for investigating the microscopic aspects of the structure of synthesized molecules. DFT is a quantum mechanical method used to investigate the electronic structure of atoms, molecules, and solids. It simplifies complex many-body interactions by focusing on electron density rather than wavefunctions. As a result, DFT provides a practical balance between computational efficiency and accuracy, making it widely used for predicting molecular properties such as charge distribution, energy levels (HOMO–LUMO), reactivity, and intermolecular interactions. Here, DFT methods were used to confirm the properties of the synthesized molecule and identify the preferred areas where anions would be interacted. The DFT would give a good result in the electronic structure between synthesized compound and anions and prediction in the transformation of the recognition event into a signal. The outcomes of these anion recognition studies can be applied to the separation and remediation of anions mixtures in industrial aqueous waste, and the production of anion sensors that can be utilized in detecting the amounts of biological anions within cells.

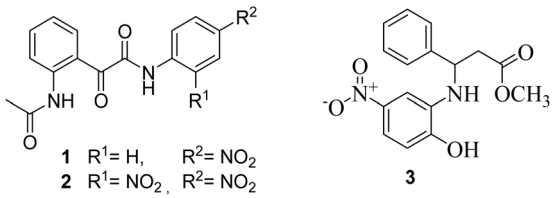

Fig. 1 *N*-Acetylglyoxylic amide derivatives (**1–2**) and cinnamaldehyde derivative bearing a nitrophenyl moiety.

Results and discussion

Synthesis of an anthracene bis-*N*-acetylglyoxylic amide derivative

Anthracence-bis-*N*-acetylglyoxylic amide **8** was designed to have amide groups in opposite position using starting materials of 1,8-diamino anthracene **6**. First, the 9,10-dibromomethylanthracene **5** was obtained from anthracene 4 with a 74% yield as a greenish solid. A singlet resonance at 5.52 ppm for the methylene protons was shown in the ^{1}H NMR spectrum of compound **5**, which was agreed with the literature values.[24] The 9,10-diaminomethylanthracene **6** was synthesized based on the procedure explained (Fig. 2).[24] The 9,10-dibromomethylanthracene **5** was reacted with tetradecyltrimethylammonium bromide in order to produce 9,10-diaminomethylanthracene **6** in 80% yield as a light brown solid. The ^{1}H NMR spectra of compound 6 matched the values found in the literature.[24]

A new compound of anthracene-bis-*N*-acetylglyoxylic amide **8** was successfully obtained in a yield of 55% by refluxing for 24 hours of 9,10-diaminomethylanthracene **6** and *N*-acetylisatin **7** in toluene (Fig. 2). The ^{1}H NMR data revealed that the synthesized compound **8** was symmetrical because just one resonance at 9.32 for the glyoxylamide N–H protons and at 10.66 ppm for amide N–H protons were spotted for each. The existence of methylene protons at 5.53 ppm was verified by a doublet.

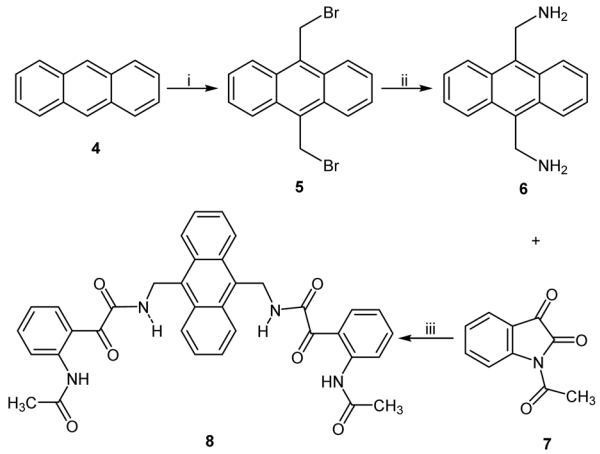

Fig. 2 Reaction steps for synthesising of an anthracene bis-*N*-acetylglyoxylic amide derivative: (i) 1,3,5-trioxane, $C_{40}H_{84}BrN$, HBr, CH_3CO_2H; (ii) hexamethylenetetramine in anhydrous $CHCl_3$ subsequently by HCl, ethanol, H_2O; (iii) toluene at reflux for 24 hours.

Studies of anion recognition by ^{1}H NMR spectroscopy

The anion binding studies of compound **8** were performed in dimethyl sulfoxide. The synthetic anthracene derivative **8**, which is poorly soluble in other aprotic media, led to the selection of this particular solvent. Fig. 3 shows partial ^{1}H NMR spectrum of compound **8** when was titrated using CN^-. This figure presents the peak changes of the aromatic, methylene, and N–H protons upon addition of CN^- solution. The ^{1}H NMR spectrum of molecule **8** is simple due to its symmetrical molecular structure. In the absence of anions, there was just one resonance for the glyoxylamide and amide N–H protons at 9.32 and 10.66 ppm, respectively. There was a doublet for the methylene protons at 5.53 ppm. The glyoxylamide and amide NH proton signals were appeared to gradually broaden, weaken, and disappear after adding 0.5–6 eq. of CN^- to solution **8**. Slightly upfield shifts for the aromatic protons of the isatin ring were found and line widening of the singlet for the $-CH_3$ protons was significantly seen, at the later titration process. The anthracene phenyl rings are not considered as potential candidates for interaction with CN^- because adding CN^- to the compound **8** solution did not modify their signals. When CN^- were present, a singlet of the methylene spacer group took the place of the doublet at 5.53 ppm. According to this data, the N–H protons in glyoxylamide were deprotonated. The findings showed that the compound **8** first coordinated with cyanide ion and when the concentration of CN^- elevated, the glyoxylamide N–H protons were then deprotonated. Two equivalents of CN^- must be added in order for the two glyoxylamide N–H protons to be deprotonated. In previous studies, an N–H group of amides serves as a binding site of chemosensor for anions.[16,17] Other studies reports that anion CN^- is connected to the host molecule by O–H and N–H, which severely inhibit the process of deprotonation.[25]

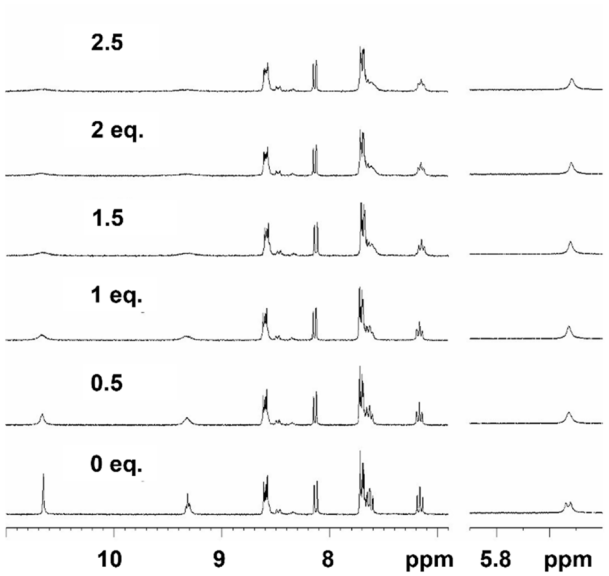

Fig. 3 The changes of compound **8** spectra upon the addition of CN^- are shown in partial ^{1}H NMR spectra.

The ^{1}H NMR spectrum shifts of compound **8** were comparable, in the case of F^-, to those of CN^-. First, when the concentration of F^- increased, the fluoride ion complexed with compound **8**, causing the N–H protons in glyoxylamide to deprotonate. The doublet at 5.53 ppm, which corresponds to the methylene protons being substituted by a singlet upon adding 2 eq. of F^-, indicates that glyoxylamide N–H protons underwent deprotonation.

The addition of 10 eq. of $H_2PO_4^-$ resulted in the glyoxylamide and amide N–H protons broadening and slightly shifting downfield. Additionally, it was observed that the methylene protons resonance was broadening. The data suggested that compound **8** and the $H_2PO_4^-$ formed hydrogen bonding interactions, while deprotonation of compound **8** was not observed. The changes NMR spectra of compound **8** upon addition of F^- and $H_2PO_4^-$ are presented in SI. On the other hand, when 10 eq. of other anions tested are added to compound **8**, the ^{1}H NMR spectrum does not change, indicating that compound **8** and these anions did not interact.

Due to their basicity, compound **8** is selective for the CN^- and F^-, allowing them to act as hydrogen bond acceptors, thereby initiate compound **8** to deprotonate. This findings aligns with a theory proposed[7] that fluoride is the smallest anion with the highest electronegativity and the ability to act as Brønsted base at increasing concentration. Similarly, at lesser concentrations, it can establish hydrogen bonds. The $H_2PO_4^-$, which has less basicity than F^- and CN^-, was the only one to form a complex with compound **8**. However, as there were only slight proton shifts noticed upon the addition of $H_2PO_4^-$, association constant data could not be acquired for this complex. Compound **8** did not interact with any of the less basic anions investigated, including Cl^-, Br^-, NO_2^-, ClO_4^-, HSO_4^-, and HPO_4^{2-}, where deprotonation did not occur.

Studies of anion recognition by UV-Vis spectroscopy

The UV-Vis absorption spectra of anthracene shows five absorption peaks at 380, 360, 343, 325, and 257 nm. These absorbance peaks are attributed to the π–π^* transition of the anthracene moiety. The structural modification for anthracene derivative **8** shifts five absorption peaks to 398, 377, 357, 339, and 262 nm (Fig. 4). Peak shifts in UV-Vis spectra often occur for molecule structural changes. The photochemical characteristics of the anthracene moieties have changed in accordance with the addition of functional groups to it. Substituents attached to the chromophore structure can shift the chromophore absorption band position and intensity. This is mostly due to changes in their electrical properties and intra- and intermolecular interactions.[26]

The interaction of compound **8** with anions was analyzed using spectrophotometric titration, which was analyzed by UV-Vis spectroscopy. When CN^- was added to the solution of **8**, there were no significant peaks changes observed in the UV-Vis spectra (Fig. 5). Moreover, once compound **8** was titrated with anions tested, no appreciable alterations were observed in its absorption spectra. Compound **8** was designed as a fluorescence Photo-induced Electron Transfer (PET) sensor/receptor,

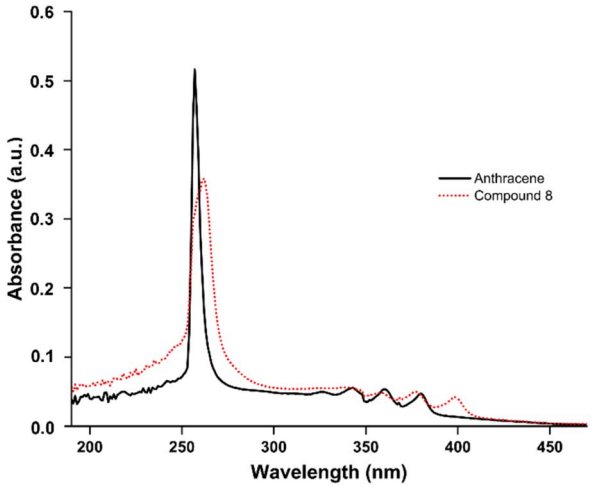

Fig. 4 The anthracene (solid) and compound **8** (dashed) absorbance spectra in dimethyl sulfoxide.

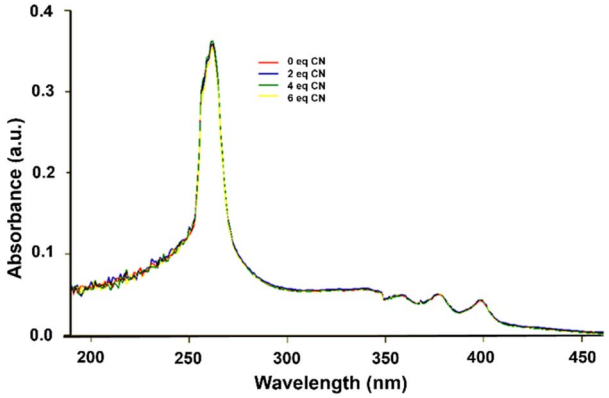

Fig. 5 The compound **8** absorbance spectra during titration with CN^- in dimethyl sulfoxide.

which consists of three important parts, such as fluorophore (anthracene), appropriate linkers (–CH_2–), and recognition/activating groups (N–H protons and the C=O (carbonyl groups)). Typical PET-based sensor/receptors are multi-component systems where a fluorophore is connected to an activating/recognition group by an unconjugated linker.[27–30] Upon addition of anions, no UV-Vis spectral change observed was the expected findings, which support the PET mechanism. The $\pi \rightarrow \pi^*$ anthracene-based absorption bands remained unchanged, which indicated that there is no considerable electronic disturbance towards anthracenyl rings due to interaction between compound **8** and anion.

Studies of anion recognition by fluorescence spectroscopy

The changes on the fluorescence emission spectrum of compound **8** was monitored during titration with anions. The fluorescence experiments were operated at 272 nm of excitation wavelength. Compound **8** demonstrated an increasing in fluorescence intensity at wavelengths of 449, 429, and 406 nm upon the addition of CN^- (0.5 eq.) (Fig. 6). Nevertheless, titrating with up to 4 eq. CN^- did not result in any additional augmentation of fluorescence intensity. The same outcomes were noted for anions of F^- in increasing the fluorescence intensity of compound **8**. Fluorescence spectra did not alter when titration with up to 4 eq. of other tested anions was carried out.

The interaction of an anthracene and an anion can either decrease or increase fluorescence. The two common mechanism of anion interaction with anthracene derivative are photoinduced electron transfer or the formation of charge-transfer complexes. Photoinduced electron transfer occurs when the presence of anions facilitates electron transfer from the excited state of anthracene derivative to the anion, resulting in fluorescence quenching. Formation of charge-transfer complexes take place when anions form complex with anthracene derivative which alter its electronic properties and increase fluorescence. Receptor protonation stabilizes the excited state. Upon excitation, an intramolecular proton transfer occurs, where a proton moves from a donor group to an acceptor group. This proton transfer stabilizes the excited state and alter the electronic structure, effectively reducing the ability of the excited state to engage in electron transfer with an anion. The suppression of PET due to intramolecular proton transfer results in increased fluorescence.[31–33]

The findings suggest that the fluorescence enhancement is attributed to the complexation of compound **8** with the CN^-, F^- or $H_2PO_4^-$. Upon initial addition of CN^- or F^-, the C=O (carbonyl groups) in compound **8** formed strong intermolecular hydrogen bonds with anion. Further addition of CN^- or F^- resulted in the protonation of compound **8**, resulting in intramolecular proton transfer and stabilizing of the excited state. Following deprotonation, no more increase in fluorescence was observed. Similarly, bis-thiocarbonohydrazones which has the anthracene fluorophore, exhibits increasing of fluorescence when F^- or AcO^- is present.[34] More detail information is presented in SI. Weaker basic anions tested, such as Cl^-, Br^-, NO_2^-, ClO_4^-, HSO_4^-, and HPO_4^{2-} are not able to form

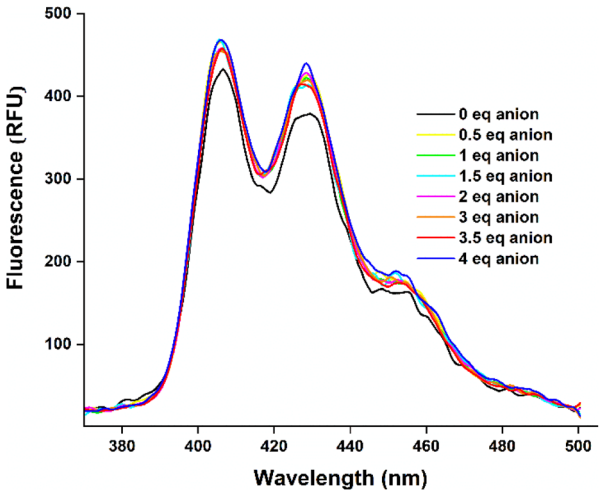

Fig. 6 The fluorescence emission spectra changes of compound **8** upon addition of CN^- in dimethyl sulfoxide.

intermolecular hydrogen bonds with the compound **8**. Therefore, for these weaker basic ions, no alterations in the fluorescence spectrum were found.

Although no significant shifts were observed in the UV-Vis absorption spectra of compound **8** upon addition of CN^-, F^-, or $H_2PO_4^-$, these results are consistent with a photoinduced electron transfer (PET) sensing mechanism. The absence of ground-state spectral changes indicates that the binding of anions does not significantly alter the electronic transitions of the anthracene core in the ground state. Instead, anion recognition appears to modulate the excited-state properties of the receptor. This is supported by the enhanced fluorescence emission, which suggests that PET from the amide donor units to the anthracene fluorophore is suppressed upon anion binding. In this way, compound **8** acts as a turn-on fluorescent sensor, where sensing relies on excited-state electronic modulation rather than ground-state perturbation, a behaviour typical of PET-based receptors.

Anion recognition studies by computational modelling

In this study, computational methods were employed to reinforce the experimental findings. The results offer a valuable starting point for understanding the receptor's behaviour and lay the groundwork for broader analyses in follow-up studies. The F^- was selected as a representative anion to model the binding interaction and to explore the charge redistribution and hydrogen bonding behaviour at the molecular level using DFT. We intended to provide an initial theoretical framework for understanding the nature of the interaction between compound **8** and the F^-. However, the gas phase of the modelled system still reflects the microscopic interactions between the two molecules involved. The lowest potential surface energy of the molecule exhibits a structure resembling a *cis*-configuration, with anthracene at its center. The molecular orbitals HOMO and LUMO of the compound are shown in Fig. 7b and c.

The electron density shifts from the anthracene donor region to the acetylglyoxylic acceptor groups. Notably, the electron density forms an extended π system within the linker section. The lowest excitation energy observed, 1.36 eV, demonstrates the transition of the electron from the HOMO to the LUMO, from the π system of anthracene to the π* system of the acetylglyoxylic group (π → π*). The highest oscillator strength (*f*) at 464.60 nm indicates the electron excitation from the π system to the π* system of the acetylglyoxylic group. Anthracene-based dyes have been investigated by Liu *et al.*, who concluded that the π → π* excitation is dominant within the range of 274.65 nm to 542.52 nm, depending on the derivative groups.[35]

Fig. 7c shows the electronic surface potential of the modeled structure (compound **8**) before and after interaction with the anion F^-. The blue area represents a more positive potential, while the yellow to red area indicates a negative surface potential. The negative surface encompasses the oxygen part, while the positive surface consists of the hydrogen part of the structure. The Electronic Potential Surface (EPS) reveals that the hydrogen atoms connected to nitrogen exhibit a higher positive

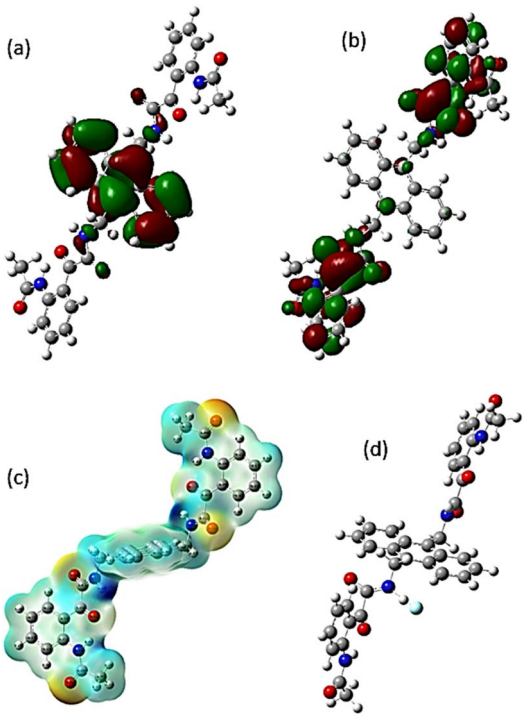

Fig. 7 Optimized structure of the compound **8** (a) HOMO orbital, (b) LUMO orbital, (c) the electronic potential surface, and (d) interaction with the anion F^-. The color represents atoms as follow grey = C, red = O, blue = N, nd white = H, ice blue = F.

charge than others, especially near the anthracene. Two regions of the acetylglyoxylic group have similar EPS. Therefore, the interaction with an anion in the positive part of one acetyl glyoxylic group can represent the interaction in the other. The interaction with the anion F^- causes the structure to relax and obtain a lower potential energy (Fig. 7d).

The structural conformation changes in response to the anion, resulting in less intramolecular hydrogen bonds. The F^- anion position tends to be close to the hydrogen of the acetyl glyoxylic group, which has a higher positive surface potential. The charge differences of the corresponding hydrogens are shown in Table 1. This Table 1 presents the properties of charge, bond distance, and electron occupancy in the interacting orbitals between the selected amine and the anion (F^-) before and after interaction. The hydrogen atom attached to nitrogen becomes more positively charged because the electron distribution in the bond changes with the elongation of the bond after interacting with the anion. As a consequence, the anion charge also decreases. The Wiberg bond index, being less than one, supports that the interaction between the hydrogens and the F^- anion has less covalent characteristics.

The NBO analysis of its natural electron configuration before and after interaction indicates elongation of the N–H bond. Upon anion binding, the increased electron occupancy in the nitrogen valence orbital reflects the accumulation of electron density near nitrogen, which is consistent with electron withdrawal from the adjacent N–H bond. This shift in electron density weakens the N–H bond, making it more susceptible to

Table 1 Properties of the interacted atoms between selected amine of the acetylglyoxylic group and the anion F^-

Properties	Before	After
NBO charge (C)		
N	−0.688	−0.750
H	0.462	0.563
F^-	−1.00	−0.731
Bond distance (Å)		
N to H	1.01	1.37
H to F^-	2.37	1.07
Wiberg bond index		
H–F^-	—	0.39
N–H	0.75	0.28
Natural electron configuration		
N	2S(1.28)2p(4.39)3p(0.01)4p(0.01)	2S(1.26)2p(4.43)4p(0.01)
H	1S(0.54)	1S(0.43)
F^-	2S(2)2p(6)	2S(1.91)2p(5.81)

deprotonation. In response, the electron occupancy in the hydrogen orbital decreases. The decrease in electrons of the F^- anion suggests electron donation to the molecules.

The non-covalent interaction of F^- with the molecules can also be concluded from the Reduced Density Gradient (RDG) isosurface. The green isosurface between the nearest atoms suggests a van der Waals interaction. As shown in Fig. 8a, the intramolecular interactions in compound 8 are rich with van der Waals interactions, confirmed by the scatter plot, which shows a green gradient with three spikes. While interacting with the F^- anion, the green gradient spike is reduced as the structural conformation changes and releases the intermolecular van der Waals interactions. However, the green isosurface point around the F^- ion confirms that the anion interacts with N–H and other nearby hydrogen atoms of the molecules. The more intense blue gradient observed at the RDG value of 0.4 to 0.6 confirms the strong attractive interaction between H and F^- by the acetylglyoxylic group (Fig. 8b). It is consistent with Mishra and Suryaprakash's work, which proves that the organic fluorine near the nearest hydrogen shows a green gradient, indicating the hydrogen bond.[36] The carbonyl oxygen atoms of compound **8** orientates the adjacent N–H groups for effective hydrogen bonding with the anion. This spatial preorganization promotes directional hydrogen bonding, where the N–H group and the anion act as a hydrogen bond donor and acceptor, respectively. Computational non-covalent interaction (NCI) analysis supports this interaction mode, highlighting localized regions of strong donor–acceptor character and the role of electrostatics in stabilizing the complexes.

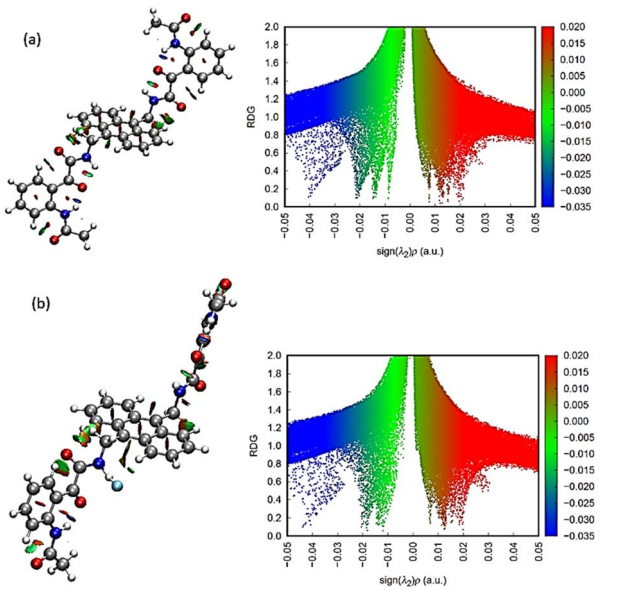

Fig. 8 Reduced Density Gradient (RDG) and scatter plot non-covalent interactions (NCI) (a) of the compound **8**, and (b) after interaction with F^-.

A single compound **8** in the gas phase was used as a model in the computational approximation, whereas in the laboratory work, the compound was present in the solution. Here, the solvent also plays a role in solvating the released proton. The elongation of the hydrogen bond when interacting with the anion can be used as justification that deprotonation is likely to occur in the next step of the reaction. As indicated by the UV data, the influence of the solvent is crucial since it causes UV peak shifting. Nevertheless, the electronic transition of compound 8 remains consistent, from the π system of anthracene to the π* system of the acetylglyoxylic group (π → π*). This has also been confirmed by data from other researchers.[35] Incorporating solvents into computational modeling significantly increases the complexity of calculations since it involves accounting for more electrons. Moreover, the complexity of UV computations increases since electron state probabilities at each level must be calculated. As a compromise, gas-phase modelling is often chosen to allow for feasible simulations using the available computer clusters.

Although detailed DFT optimization was performed primarily for the F^- complex, comparative insights can also be inferred for CN^- and $H_2PO_4^-$ based on their observed binding behaviour and known electronic properties. Both CN^- and F^- act as strong bases, and their addition resulted in receptor deprotonation experimentally. This suggests that these anions first interact electrostatically with the amide moiety's acidic N–H protons before abstracting protons. In contrast, $H_2PO_4^-$, a weaker base and a better hydrogen bond donor/acceptor, generated a stable complex without deprotonation, possibly through a network of hydrogen bonds involving both the amide and carbonyl groups. These differing modes of interaction supports the receptor's selective fluorescence enhancement due to increased rigidity or binding-induced conformational changes.

The selective fluorescence enhancement of compound **8** in response to CN^-, F^-, and $H_2PO_4^-$ indicates strong potential for practical sensing applications. In particular, it may be useful for monitoring hazardous anions in industrial wastewater, where rapid and selective detection is required. Furthermore, the receptor's turn-on fluorescence behaviour suggests suitability

for intracellular imaging of biologically relevant anions such as phosphate species. With further modifications to improve water solubility and biocompatibility, this receptor could be used for environmental and medicinal applications, such as incorporation into solid-state or nanomaterial-based sensing platforms. While this study provides meaningful insight into the selective recognition of anions by the synthesized anthracene-bis-*N*-acetylglyoxylic amide receptor, limitations should be addressed. DFT calculations were conducted in the gas phase and do not fully capture solvent effects—an important factor in anion recognition under aqueous or polar conditions. The absence of solvation models may result in discrepancies between theoretical predictions and experimental observations. However, gas-phase modeling remains valuable in the early stages of receptor design, allowing rapid screening of multiple candidates before committing to more computationally demanding solution-phase studies. Additionally, by omitting solvent effects, gas-phase calculations highlight the intrinsic electronic and structural features of receptor–anion interactions, providing a clearer understanding of the fundamental binding behaviour.

Experimental

Materials

Chemicals were purchased from E-Merck, such as anthracene, 1,3,5-trioxane, isatin, tetradecyltrimethylammonium bromide, tetrabutylammonium salt, hydrobromic acid, hydrochloric acid, glacial acetic acid, chloroform, ethanol, and potassium bicarbonate.

Synthesis of 9,10-bis-(bromomethyl)anthracene 5

A solution of glacial acetic acid (25 mL) and 48% HBr (100 mL) was used to dissolve anthracene **4** (28 mmol, 5 g). The following chemicals were added: 1,3,5-trioxane (64 mmol, 5 g) and 0.2 g of tetradecyltrimethylammonium bromide. The reaction mixture was brought at reflux while being stirred for 24 hours. After cooling, the resultant precipitate was collected, cleaned with ethanol and water, and then recrystallized from toluene to give 7.58 g of a greenish solid **5** in 74% yield. M.p. 300 °C (lit. 300 °C);[22] ^{1}H NMR (300 MHz, DMSO-d_6): δ 5.52 (s, 4H, 2 × CH_2), 7.68 (dd, J = 6.8, 3.3 Hz, 4H, ArH), 8.37 (dd, J = 6.9, 3.2 Hz, 4H, ArH). The values in the literature and the ^{1}H NMR data confirmed.[24]

Synthesis of 9,10-bis-(aminomethyl)anthracene 6

A solution of hexamethylenetetramine (2.03 mmol, 0.2848 g) in anhydrous chloroform (10 mL) was mixed dropwise with 10-bromomethylanthracene **5** (1.02 mmol, 0.37 g) in anhydrous chloroform (15 mL). Reflux was applied to the reaction mixture for 5 hours. After a while, the precipitate was obtained and cleaned with water. A solution of strong hydrochloric acid, ethanol, and water (5 : 20 : 4) was mixed with the resultant solid. The reaction mixture was brought at 70 °C overnight. After one hour, the resultant precipitate re-precipitated out of solution after first dissolving. The resultant precipitate was gathered, mixed with 10% potassium bicarbonate (20 mL), and then extracted twice into 20 mL of chloroform. The organic layer was reduced *in vacuo* and dried with magnesium sulfate to provide 0.19 g of the light brown solid in 80% yield as compound **6**. M.p. 234–236 °C (Lit. 238 °C);[22] ^{1}H NMR (300 MHz, DMSO-d_6): δ 4.69 (s, 4H, 2 × CH_2), 7.58 (dd, J = 7.0, 3.2 Hz, 4H, ArH), 8.47 (dd, J = 6.8, 3.2 Hz, 4H, ArH). The values in the literature and the ^{1}H NMR results agreed.[24]

Synthesis of *N*,*N*′-(anthracene-9,10-diylbis(methylene))bis(2-(2-acetamidophenyl)-2-oxoacetamide) 8

Compound 9,10-diaminomethylanthracene **6** (0.66 mmol, 0.16 g) was added to an agitated *N*-acetylisatin **7** solution (1.32 mmol, 0.25 g) in toluene (30 mL). The reaction mixture was heated for 24 hours at reflux. A greenish solid **8** (0.22 g) was obtained by re-crystallizing the precipitate from methanol in 55% yield. M.p. 280–282 °C; UV(DMSO): λ_{max} 262 (ε 218 174 cm^{-1} M^{-1}), 341 (31 300), 358 (33 800), 337 (38 500), 339 (36 450); IR (KBr): ν_{max} 3275, 3071, 2923, 1694, 1644, 1608, 1584, 1527, 1449, 1365, 1321, 1283, 1205, 1130, 1031, 954, 864, 752 cm^{-1}; ^{1}H NMR (300 MHz, DMSO-d_6): δ 1.99 (s, 6H, COC$\underline{H}_3$), 5.53 (d, J = 5.3 Hz, 4H, 2 × C$\underline{H}_2$NHCO), 7.14–7.19 (m, 2H, ArH), 7.60–7.72 (m, 8H, ArH), 8.14 (dd, J = 8.4, 0.7 Hz, 2H, ArH), 8.59 (dd, J = 6.9, 3.3 Hz, 4H, ArH), 9.32 (t, J = 5.3 Hz, 1H, 1 × N$\underline{H}$ CO), 10.66 (s, 1H, 1 × NHCO); ^{13}C NMR (75 MHz, DMSO-d_6): δ 24.7 (2 × CO$\underline{C}$ H_3), 35.5, 121.4 (2 × $\underline{C}$ H_2NHCO), 122.0, 130.3, 130.5, 139.9 (10 × ArC), 123.6, 125.6, 126.6, 132.8, 135.4 (16 × ArCH), 164.8, 169.5, 193.1 (6 × C═O); HRMS (ESI) m/z calculated for $C_{36}H_{30}N_4O_6Na$ $(M + Na)^+$ 637.2048. Found 637.2058; anal. calcd. for $C_{36}H_{30}N_4O_6$: C, 70.35; H, 4.92; N, 9.12. Found: C, 70.24; H, 4.96; N, 8.85%.

Studies of anion recognition by NMR, UV-Vis, and fluorescence spectroscopy

Titration studies were carried out by gradually adding a standard solution containing compound **8** and an anion (as its tetrabutylammonium salt) in order to maintain the concentration of compound **8** constant. The anion used was F^-, Cl^-, Br^-, CN^-, $H_2PO_4^-$, NO_2^-, ClO_4^-, HSO_4^-, or HPO_4^{2-}. Using a Bruker AVANCE DPX300 (300 MHz) spectrometer was used to obtain NMR spectra. A Varian Cary 100 Scan spectrometer was used to record ultraviolet-visible spectra. A Cary Eclipse Fluorescence spectrometer was used to get fluorescence spectra.

Studies of anion recognition by computational modelling

The anthracence-bis-*N*-acetylglyoxylic amide **8** was fully relaxed. Initial optimization was performed using the B3LYP level of DFT with the 6-31G(d) basis set, followed by refinement at the B2PLYPD3/6-31+G(d,p) level to better capture interactions with anionic species and include solvation effects in the calculations. To ensure the structure has the lowest energy once optimized structure is found, a conformational search of the derivate structure was done around 0–180° in 18 steps of 10. The proper and lowest energy of the conformed structure is then reoptimized until the calculation convergent. Complete optimization has also been performed for certain selected minima to locate the actual minimum on the potential energy surface. The lowest

energy state is verified by the occurrence of zero imaginary frequencies. The TDDFT was employed to observed the electron excitation of the lowest energy structure. All quantum chemical computations were solved using Gaussian 16.[37]

The physical adsorption of anions onto the adsorbent surface occurs *via* weak interactions like electrostatic forces, hydrogen bonding, hydrophobic effects, and van der Waals attractions. For proteins, the anions are attracted to positively charged areas on the surface. Here, the interaction involving the F^- anion was suggested to occur near the positively charged surface region of the molecule.[38,39] The reaction involving the F^- anion was suggested to occur near the positively charged surface region of the molecule. The interaction between modeled structures and the anion was facilitated by placing the anion near the amide group, which has a more positively charged hydrogen atom. There were two similar potential sites; only one was chosen to represent the interaction with the anion. The molecular structure was optimized using a method similar to those used before the interaction. The atomic Mulliken charge, natural bond orbital (NBO) analysis,[40] and reduced density gradient (RDG) of the Non-Covalent Interaction analysis (NCI) method were utilized to examine the correlation between the interaction and electronic properties of the corresponding compound with the F^- anion.

Dispersion corrections are crucial for highly conjugated molecules, such as graphene and graphite, and for large, flexible structures. For less conjugated molecules, the energy discrepancies without dispersion corrections remain acceptable. The optimized geometries and electronic properties of anthracene derivatives, computed using the B3LYP functional with the appropriate basis set, align well with experimental data. This has been extensively explored in prior studies, where anthracene and its derivatives were modeled using DFT, particularly with the B3LYP method.[41–45]

Conclusions

The anthracene-bis-*N*-acetylglyoxylic amide anthracene **8** was obtained by reacting the 9,10-diaminomethylanthracene and *N*-acetylisatin. Compound **8** exhibited a selective recognition for CN^-, F^-, and $H_2PO_4^-$. Compound **8** and $H_2PO_4^-$ formed a complex by intermolecular hydrogen bonding linkages. The addition of these anions resulted in increase in fluorescence intensity, which was explained by intramolecular proton transfer in compound **8**. The DFT investigation reveals that the interaction occurs through the hydrogen atom of the acetylglyoxylic and an anion F^-. The non-covalent type interaction is dominant based on its electronic properties, which is further supported by the NCI analysis. The results of our studies contribute an important insight into the anion recognition by glyoxylic amide receptor bearing anthracene fluorescence subunit. Beyond fundamental insight, these findings suggest promising applications for compound **8** in anion sensing in industrial wastewater, where CN^- and F^- contamination is a concern, and potentially in intracellular anion imaging, given the fluorescence enhancement mechanism. Future development of this receptor for real-world matrices could broaden its relevance in environmental and biomedical contexts.

Author contributions

VS performed the synthesis and spectroscopic characterization, conceived the study, contributed to data interpretation, and finalized the manuscript. HAS performed the synthesis and spectroscopic characterization, and drafted the initial manuscript. YH contributed to computational (DFT) studies, data analysis, and interpretation of molecular interaction results. DB provided conceptual guidance, critical revisions, and scientific advice throughout the project. NK assisted in experimental design, contributed to spectroscopic data interpretation, and helped revise the manuscript. All authors reviewed and approved the final manuscript.

Conflicts of interest

There are no conflicts to declare.

Data availability

The datasets supporting the findings of this study, including raw data, processed data, and supplementary materials, can be obtained from the corresponding author upon reasonable request.

Acknowledgements

The authors would like to thank the Indonesian Endowment Fund for Education Agency (LPDP) under the DAPT Equity Program of Universitas Sebelas Maret 2023/2024 with contract number: 3272.1/UN27.22/PT.01.03/2023.

References

1 L. K. Macreadie, A. M. Gilchrist, D. A. McNaughton, W. G. Ryder, M. Fares and P. A. Gale, Progress in anion receptor chemistry, *Chem*, 2022, **8**, 46–118.
2 L. Chen, S. N. Berry, X. Wu, E. N. W. Howe and P. A. Gale, Advances in anion receptor chemistry, *Chem*, 2020, **6**, 61–141.
3 G. Picci, R. Montis, V. Lippolis and C. Caltagirone, Quaramide-based receptors in anion supramolecular chemistry: insights into anion binding, sensing, transport and extraction, *Chem. Soc. Rev.*, 2024, **53**, 3952–3975.
4 R. Plais, G. Clavier, J. Y. Salpin, A. Gaucher and D. Prim, Anion-π interaction for molecular recognition of anions: focus on cooperativity with hydrogen bonding, *Eur. J. Org. Chem.*, 2023, **26**, e202201281.
5 D. Barišić, F. Lešić, M. Tireli Vlašić, K. Užarević, N. Bregović and V. Tomišić, Anion binding by receptors containing NH donating groups – what do anions prefer?, *Tetrahedron*, 2022, **120**, 132875.

6 X. Chen, Y. Pan, T. Tang, J. Fu, X. Chen and C. Bao, Machine learning-guided one-step fabrication of targeted emodin liposomes via novel micromixer for ulcerative colitis therapy, *Nano Res.*, 2025, **18**, 94907713.
7 X. Chen, J. Zhai and X. Chen, A novel micromixer based on coastal fractal for manufacturing controllable size liposome, *Phys. Fluids*, 2024, **36**, 112009.
8 X. Chen, T. Tang, J. Zhai, X. Li and X. Chen, Bioinspired Leaf-Vein Micromixer for a Rapid and Efficient Synthesis of Monodisperse Ciprofloxacin Lipid Nanoparticles, *Langmuir*, 2025, **41**, 19572–19581.
9 L. Chen, S. N. Berry, X. Wu, E. N. W. Howe and P. A. Gale, Advances in anion receptor chemistry, *Chem*, 2020, **6**, 61–141.
10 C. L. Ritt, M. Liu, T. A. Pham, R. Epsztein and H. J. Kulik, Machine learning reveals key ion selectivity mechanisms in polymeric membranes with subnanometer pores, *Sci. Adv.*, 2022, **8**, eabl5771.
11 D. A. McNaughton, W. G. Ryder, A. M. Gilchrist, P. Wang, M. Fares, X. Wu and P. A. Gale, New insights and discoveries in anion receptor chemistry, *Chem*, 2023, **9**, 3045–3112.
12 X. Cheng, B. Feng, F. Chen, S. Huang, S. Zhang and F. Gao, Development of a water-soluble fluorescent probe based on natural flavylium for mercury(II) ion detection and clinical antidote evaluation, *J. Agric. Food Chem.*, 2023, **71**, 13263–13269.
13 A. Joshi, N. Mukherjee and M. Pandey, Water-soluble organic fluorescence-based probes for biomolecule sensing and labeling, *Biosens. Bioelectron.: X*, 2024, **19**, 100510.
14 V. Suryanti, G. C. Condie, M. Bhadbhade, R. Bishop, D. S. C. Black and N. Kumar, Synthesis, structures, and conformations of linked bis-glyoxylamides derived from bis-acylisatins, *Aust. J. Chem.*, 2014, **67**, 1270–1278.
15 V. Suryanti, R. Zhang, V. Aldilla, M. Bhadbhade, N. Kumar and D. S. Black, Synthesis of bis-glyoxylamide peptidomimetics derived from bis-n-acetylisatins linked at C5 by a methylene or oxygen bridge, *Molecules*, 2019, **24**, 1–15.
16 V. Suryanti, M. Bhadbhade, D. S. C. Black and N. Kumar, N-Acetylglyoxylic amide bearing a nitrophenyl group as anion receptors: NMR and X-ray investigations on anion binding and selectivity, *J. Mol. Struct.*, 2017, **1146**, 571–576.
17 V. Suryanti, M. Bhadbhade, H. M. Chawla, E. Howe, P. Thordarson, D. S. C. Black and N. Kumar, Novel colorimetric anion sensors based on N-acetylglyoxylic amides containing nitrophenyl signalling units, *Spectrochim. Acta, Part A*, 2014, **121**, 662–669.
18 V. Suryanti, F. R. Wibowo and S. Handayani, Methyl-3-(2-hydroxy-5-nitrophenyl amino)-3-phenylpropanoate based colorimetric sensor for oxyanions, *Indones. J. Chem.*, 2020, **20**, 257–263.
19 V. Suryanti, F. R. Wibowo, A. Marzuki and M. R. K. Sari, Cation sensing capabilities of a nitrophenyl cinnamaldehyde derivative, *Molekul*, 2020, **15**, 191–198.
20 B. S. Morozov, S. S. R. Namashivaya, M. A. Zakharko, A. S. Oshchepkov and E. A. Kataev, Anthracene-Based Amido–Amine Cage Receptor for Anion Recognition under Neutral Aqueous Conditions, *ChemistryOpen*, 2020, **9**, 171–175.
21 M. Zaleskaya-hernik, Ł. Dobrzycki, M. Karbarz and J. Romański, Fluorescence recognition of anions using a heteroditopic receptor: homogenous and two-phase sensing, *Int. J. Mol. Sci.*, 2021, **22**, 13396.
22 C. M. G. Dos Santos, M. Glynn, T. McCabe, J. S. S. De Melo, H. D. Burrows and T. Gunnlaugsson, Synthesis, structural and photophysical evaluations of urea based fluorescent PET sensors for anions, *Supramol. Chem.*, 2008, **20**, 407–418.
23 T. Gunnlaugsson, M. Glynn, G. M. Tocci (née Hussey), P. E. Kruger and F. M. Pfeffer, Anion recognition and sensing in organic and aqueous media using luminescent and colorimetric sensors, *Coord. Chem. Rev.*, 2006, **250**, 3094–3117.
24 T. Gunnlaugsson, A. P. Davis, J. E. O'Brien and M. Glynn, Synthesis and photophysical evaluation of charge neutral thiourea or urea based fluorescent PET sensors for bis-carboxylates and pyrophosphate, *Org. Biomol. Chem.*, 2005, **3**, 48–56.
25 T. P. Martyanov, A. A. Kudrevatykh, E. N. Ushakov, D. V. Korchagin, I. V. Sulimenkov, S. G. Vasil'ev, S. P. Gromov and L. S. Klimenko, Selective colorimetric sensor for cyanide anion based on 1-hydroxyanthraquinone, *Tetrahedron*, 2021, **93**, 132312.
26 A. Kastrati, F. Oswald, A. Scalabre and K. M. Fromm, Photophysical Properties of Anthracene Derivatives, *Photochem*, 2023, **3**, 227–273.
27 N. Kaur and B. Kaur, Recent development in anthracene possessing chemosensors for cations and anions, *Microchem. J.*, 2020, **158**, 105131.
28 M. H. Nguyen, T. N. Nguyen, D. Q. Do, H. H. Nguyen, Q. M. Phung, N. Thirumalaivasan, S. P. Wu and T. H. Dinh, A highly selective fluorescent anthracene-based chemosensor for imaging Zn^{2+} in living cells and zebrafish, *Inorg. Chem. Commun.*, 2020, **115**, 107882.
29 R. Martínez-Máñez and F. Sancenón, New advances in fluorogenic anion chemosensors, *J. Fluoresc.*, 2005, **15**, 267–285.
30 T. Gunnlaugsson, A. P. Davis, G. M. Hussey, J. Tierney and M. Glynn, Design, synthesis and photophysical studies of simple fluorescent anion PET sensors using charge neutral thiourea receptors, *Org. Biomol. Chem.*, 2004, **2**, 1856–1863.
31 D. Aigner, S. A. Freunberger, M. Wilkening, R. Saf, S. M. Borisov and I. Klimant, Enhancing photoinduced electron transfer efficiency of fluorescent pH-probes with halogenated phenols, *Anal. Chem.*, 2014, **86**, 9293–9300.
32 N. I. Georgiev, V. V. Bakov and V. B. Bojinov, Photoinduced Electron Transfer and Aggregation-Induced Emission in 1,8-Naphthalimide Probes as a Platform for Detection of Acid/Base Vapors, *Photonics*, 2022, **9**, 994.
33 H. Niu, J. Liu, H. M. O'Connor, T. Gunnlaugsson, T. D. James and H. Zhang, Photoinduced electron transfer (PeT) based fluorescent probes for cellular imaging and disease therapy, *Chem. Soc. Rev.*, 2023, **52**, 2322–2357.

34 F. Han, Y. Bao, Z. Yang, T. M. Fyles, J. Zhao, X. Peng, J. Fan, Y. Wu and S. Sun, Simple bisthiocarbonohydrazones as sensitive, selective, colorimetric, and switch-on fluorescent chemosensors for fluoride anions, *Chem.–Eur. J.*, 2007, **13**, 2880–2892.

35 Q. Liu, Q. Wang, M. Xu, J. Liu and J. Liang, DFT characterization and design of anthracene-based molecules for improving spectra and charge transfer, *Spectrochim. Acta, Part A*, 2020, **227**, 117627.

36 S. K. Mishra and N. Suryaprakash, Intramolecular hydrogen bonding involving organic fluorine: NMR investigations corroborated by DFT-based theoretical calculations, *Molecules*, 2017, **22**, 1–44.

37 M. J. Frisch, G. W. Trucks, H. B. Schlegel, G. E. Scuseria, M. A. Robb, J. R. Cheeseman, G. Scalmani, V. Barone, G. A. Petersson, H. Nakatsuji, X. Li, M. Caricato, A. Marenich, J. Bloino, B. G. Janesko, R. Gomperts, B. Mennucci, H. P. Hratchian, J. V. Ortiz and D. J. Fox, *Gaussian 09, Revision A.09*, Gaussian, Inc., Wallingford, E.U.A., 2016.

38 A. C. Marques, P. J. Costa, S. Velho and M. H. Amaral, Functionalizing nanoparticles with cancer-targeting antibodies: a comparison of strategies, *J. Controlled Release*, 2020, **320**, 180–200.

39 B. Yu, C. C. Pletka and J. Iwahara, Quantifying and visualizing weak interactions between anions and proteins, *Proc. Natl. Acad. Sci. U. S. A.*, 2021, **118**, e32015879118.

40 F. Weinhold, Natural bond orbital analysis: a critical overview of relationships to alternative bonding perspectives, *J. Comput. Chem.*, 2012, **33**, 2363–2379.

41 A. Gümüş, V. Okumuş and S. Gümüş, Synthesis, biological evaluation of antioxidant-antibacterial activities and computational studies of novel anthracene- and pyrene-based Schiff base derivatives, *Turk. J. Chem.*, 2020, **44**, 1200–1215.

42 Z. T. İrak, A. Gümüş and S. Gümüş, Investigation of TADF properties of novel donor-acceptor type pyrazine derivatives, *J. Chil. Chem. Soc.*, 2019, **64**, 4303–4309.

43 J. Jebasingh Kores, I. Antony Danish, T. Sasitha, J. Gershom Stuart, E. Jimla Pushpam and J. Winfred Jebaraj, Spectral, NBO, NLO, NCI, aromaticity and charge transfer analyses of anthracene-9,10-dicarboxaldehyde by DFT, *Heliyon*, 2021, **7**, e08377.

44 P. S. Patil, S. R. Maidur, J. R. Jahagirdar, T. S. Chia, C. K. Quah and M. Shkir, Crystal structure, spectroscopic analyses, linear and third-order nonlinear optical properties of anthracene-based chalcone derivative for visible laser protection, *Appl. Phys. B: Lasers Opt.*, 2019, **125**, 1–13.

45 D. A. Zainuri, I. A. Razak and S. Arshad, Molecular structure, DFT studies and Hirshfeld analysis of anthracenyl chalcone derivatives, *Acta Crystallogr., Sect. E: Crystallogr. Commun.*, 2018, **74**, 780–785.